arXiv:1411.2970v4 [astro-ph.CO] 20 Sep 2016

Response function of the large-scale structure of the universe to the small scale inhomogeneities

Takahiro Nishimichi[a,c,d,*], Francis Bernardeau[a,b], Atsushi Taruya[e,c]

[a] *Sorbonne Universités UPMC Univ Paris 6 et CNRS, UMR 7095, Institut dAstrophysique de Paris, 98 bis bd Arago 75014 Paris, France*
[b] *CEA - CNRS, UMR 3681, Institut de Physique Théorique, F-91191 Gif-sur-Yvette, France*
[c] *Kavli Institute for the Physics and Mathematics of the Universe (WPI), The University of Tokyo Institutes for Advanced Study, The University of Tokyo, 5-1-5 Kashiwanoha, Kashiwa 277-8583, Japan*
[d] *CREST, JST, 4-1-8 Honcho, Kawaguchi, Saitama, 332-0012, Japan*
[e] *Yukawa Institute for Theoretical Physics, Kyoto University, Kyoto 606-8502, Japan*

Abstract

In order to infer the impact of the small-scale physics to the large-scale properties of the universe, we use a series of cosmological N-body simulations of self-gravitating matter inhomogeneities to measure, for the first time, the response function of such a system defined as a functional derivative of the nonlinear power spectrum with respect to its linear counterpart. Its measured shape and amplitude are found to be in good agreement with perturbation theory predictions except for the coupling from small to large-scale perturbations. The latter is found to be significantly damped, following a Lorentzian form. These results shed light on validity regime of perturbation theory calculations giving a useful guideline for regularization of small scale effects in analytical modeling. Most importantly our result indicates that the statistical properties of the large-scale structure of the universe are remarkably insensitive to the details of the small-scale physics, astrophysical or gravitational, paving the way for the derivation of robust estimates of theoretical uncertainties on the determination of cosmological parameters from large-scale survey observations.

Keywords: Gravitational growth of cosmic structures, Perturbation theory, N-body simulation

1. introduction

The cosmic energy fluctuations on large scales provide rich probes of the early universe physics, the mass of neutrinos or the nature of dark energy. Wide-field galaxy surveys are therefore widely considered for unveiling the details of

*Corresponding author

the universe [1]. Among them are the DES[1], LSST[2] and Euclid[3] now under development. Such measurements rely however largely on our understanding of the statistical properties of the cosmic fluctuations. The great success of the latest cosmic microwave background observations in establishing the standard picture of our Universe largely owed to the fact that the measured temperature fluctuations are in the linear regime and thus can accurately be predicted using linear theory [2, 3]. Likewise, we expect that the late-time fluctuations on large scales are in a mildly nonlinear stage, and there are robust ways to predict them precisely beyond linear-theory calculations.

Established probes such as the baryon acoustic oscillations (BAOs; e.g. [4, 5]) that give us a robust standard ruler useful for dark energy studies, or the redshift-space distortions (e.g., [6]) as an additional clue to discriminate gravity theories [7], are among those that we expect in a mildly nonlinear regime. Alternatively, we can access cosmic fluctuations on similar and somewhat smaller scales with weak-lensing measurements (see [8] for a recent review). Such scientific programs can only be achieved if related observables can be accurately predicted either from numerical simulations or analytically for any given cosmological model. In particular it is important that such observables are shielded from the details of astrophysics at galactic or sub-galactic scales [4].

One way to reformulate this question is to quantify the impact of small-scale structures on the growth of large scale modes. Perturbation theory (PT) is a powerful framework to predict the growth of structure. Assuming that the system is described by self-gravitating pressure-less fluids, it provides the first-principle approach to the nonlinear growth (see [12] for a review). Its importance has been heightened after the detection of BAOs in the clustering of galaxies, making precise predictions of nonlinearities crucially important.

PT calculations show precisely that mode couplings between different scales are unavoidable. We propose here to quantify these couplings with a two-variable response function [5], defined as the linear response of the *nonlinear* power spectrum at wave mode k with respect to the *linear* counterpart at wave mode q [6]:

$$K(k,q;z) = q\frac{\delta P^{\rm nl}(k;z)}{\delta P^{\rm lin}(q;z)}. \tag{1}$$

In the context of PT calculations, [14, 15] showed progressive broadening of the

[1] https://www.darkenergysurvey.org/

[2] http://www.lsst.org/lsst/

[3] http://www.euclid-ec.org

[4] For instance in [9, 10, 11] baryonic effects are shown to be confined within the cluster scale, and they contribute to the matter power spectrum at most $\sim 10\%$ at $k = 1\,h\,{\rm Mpc}^{-1}$ and drops rapidly toward larger scales.

[5] This concept was recently utilized in Ref. [13] to compute the difference of the nonlinear power spectrum for slightly different cosmological models.

[6] The normalization is such that K contributes to the change in $P^{\rm nl}$ with uniform weights per decade.

response function with increasing PT order, pointing to the need of regularization of the small-scale contribution.

If the broadness of the response function at late times is true, physics at very small scale can influence significantly the matter distribution on large scales, where the acoustic feature is prominent [7]. It also questions the reliability of simulations, which can follow the evolution of Fourier modes only in a finite dynamical range. We here discuss the response function at the non-perturbative level utilizing cosmological N-body simulations.

2. Methodology

We here describe our method to measure the response function from simulations. We prepare two initial conditions with small modulations in the linear spectrum over a finite interval of wave mode q, evolve them to a late time, and take the difference of the nonlinear spectra measured from the two. That is

$$\hat{K}_{i,j}P_j^{\rm lin} \equiv \frac{P_i^{\rm nl}[P_{+,j}^{\rm lin}] - P_i^{\rm nl}[P_{-,j}^{\rm lin}]}{\Delta\ln P^{\rm lin}\Delta\ln q}, \tag{2}$$

where the two perturbed linear spectra are given by

$$\ln\left[\frac{P_{\pm,j}^{\rm lin}(q)}{P^{\rm lin}(q)}\right] = \begin{cases} \pm\dfrac{1}{2}\Delta\ln P^{\rm lin} & \text{if } q\in[q_j,q_{j+1}), \\ 0 & \text{otherwise.} \end{cases} \tag{3}$$

In the above, the index i (j) runs over the wave-mode bins for the nonlinear (linear) spectrum, and we choose log-equal binning, $\ln q_{j+1} - \ln q_j = \ln k_{i+1} - \ln k_i = \Delta\ln q$. It is straightforward to show that the estimator $\hat{K}$ approaches to the response function K defined in Eq. (1), when $\Delta\ln q$ and $\Delta\ln P^{\rm lin}$ are small. The definition (1) is advantageous in that it allows the measurement in this way at the fully nonlinear level [8]. Note that a similar function was first discussed numerically in Ref. [18] in the context of local transformations of the density field.

We adopt a flat-ΛCDM cosmology consistent with the five-year WMAP result [19] with parameters $(\Omega_{\rm m}, \Omega_{\rm b}/\Omega_{\rm m}, h, A_{\rm s}, n_{\rm s}) = (0.279, 0.165, 0.701, 2.49\times 10^{-9}, 0.96)$, which are the current matter density parameter, baryon fraction, the Hubble constant in units of $100km/s/$Mpc, the scalar amplitude normalized at $k_0 = 0.002{\rm Mpc}^{-1}$ and its power index, respectively. We also consider different cosmologies to check the generality of the result. Since we can check the dependence of the response function on the overall amplitude of the power spectrum by looking at the results at different redshifts, we here focus on the variety in only the shape of the spectrum. As a representative of the parameters that control the shape, we consider the spectral tilt $n_{\rm s}$. We run simulations for two

[7] Notice, however, that the feature can also be affected by galaxy bias [16, 17].
[8] This is contrasted to the function F_n appearing in PT for the n-th order coupling.

additional models, one with a higher (1.21; `high_ns`) and the other with a lower (0.71; `low_ns`) value of $n_{\rm s}$. Although the parameter $n_{\rm s}$ has been constrained very tightly from observations of the cosmic microwave background (with only $\sim 1\%$ uncertainty), we choose to give it a rather large (± 0.25) variation to cover a wider class of models with different linear power spectra. The amplitude parameter $A_{\rm s}$ for these models are determined such that the rms linear fluctuation at $8\,h^{-1}$Mpc is kept unchanged. The matter transfer function is computed for these models using the `CAMB` code [20] with the high-precision mode of the calculation in the transfer function (`transfer_high_precision` is set to be true and `accuracy_boost`$= 2$) up to $k_{\rm max} = 100\,h\,{\rm Mpc}^{-1}$. We confirm that the result is well converged by testing more strict values in the parameter file.

We run four sets of simulations for the fiducial model with different volume and number of particles as listed in Table 1. Covering different wave number intervals, these simulations allow us to examine the convergence of the measured response function. The initial conditions are created using a code developed in [21, 22] based on the second-order Lagrangian PT (e.g., [23, 24]). The initial redshifts of the simulations are determined as follows. A lower starting redshift can induce transient effects associated with higher-order decaying modes. On the other hand, as increasing the initial redshift, the randomly generated particle position generally gets closer to the pre-initial grid, and this can lead to discreteness noise in the force calculation. To minimize the sum of these two systematic effects, we set the initial redshift such that the rms displacement is roughly 20% of the inter-particle spacing, and thus it depends on the resolution as shown in Table 1. We evolve the matter distribution using a Tree-PM code `Gadget2` [25]. We finally measure the power spectrum by fast Fourier transform of the Cloud-in-Cell (CIC) density estimates on 1024^3 mesh with the CIC kernel deconvolved in Fourier space.

For each set of simulations, we prepare multiple initial conditions with linear spectra perturbed by $\pm 1\%$ over $q_j \le q < q_{j+1}$. The amplitude of perturbation should be sufficiently small such that the correction from the higher-order derivative ($\delta^2 P^{\rm nl}/\delta P^{\rm lin}\delta P^{\rm lin}$) does not contaminate the result. We tested different amplitudes ($\pm 3\%$ and $\pm 5\%$), and confirmed that the result is almost unchanged. We set the bin width as $\Delta \ln q = \ln(\sqrt{2})$ and each simulation set covers different wavenumber range corresponding to the box size and resolution limit. The binning effect will be taken into account in the analytical calculations for fair comparison. For the best resolution run, `L9-N10`, we study only five bins on small scales. Further, we perform four realizations for `L9-N9` and `L9-N8` at each wave-mode bin to estimate the statistical scatter. The same random phases are used for initial conditions with positive and negative perturbations at each q bins for each realization. Since the estimator (2) takes the difference of the two spectra, this helps us to reduce the statistical scatter on the response function significantly.

Table 1: Simulation parameters. Box size (box), softening scale (soft) and mass of the particles (mass) are respectively given in unit of h^{-1}Mpc, h^{-1}kpc and $10^{10}h^{-1}M_\odot$. The number of q-bins is shown in the "bins" column, for each of which we run two simulations with positive and negative perturbations in the linear spectrum. The "runs" column shows the number of independent initial random phases over which we repeat the same analysis. The total number of simulations are shown in the "total" column.

name	box	particles	$z_{\rm start}$	soft	mass	bins	runs	total
`L9-N10`	512	1024^3	63	25	0.97	5	1	10
`L9-N9`	512	512^3	31	50	7.74	15	4	120
`L9-N8`	512	256^3	15	100	61.95	13	4	104
`L10-N9`	1024	512^3	15	100	61.95	15	1	30
`high_ns`	512	512^3	31	50	7.74	5	4	40
`low_ns`	512	512^3	31	50	7.74	5	4	40

3. Shape of the response function and comparison with PT

We are now in a position to present the response function measured from simulations. The combination $K(k,q)P^{\rm lin}(q)$ is plotted at a fixed k shown by the vertical arrow as a function of q in Fig. 1. The strong overlap among different symbols and lines ensures the convergence of the results against resolution and volume.

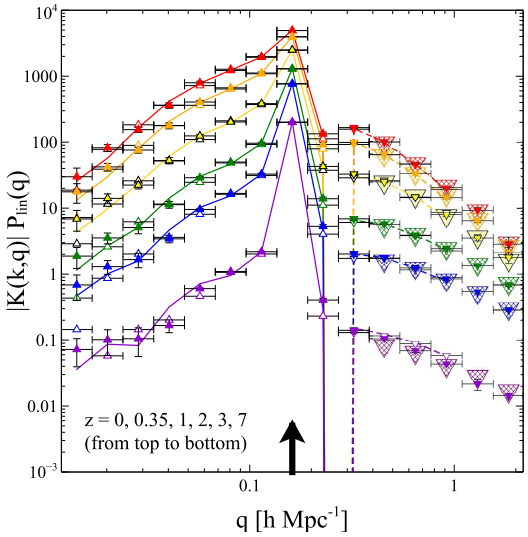

Figure 1: Response function measured from simulations. We plot $|K(k,q)|P^{\rm lin}(q)$ as a function of the linear mode q for a fixed nonlinear mode at $k = 0.161\,h\,{\rm Mpc}^{-1}$ indicated by the vertical arrow. The filled (open) symbols show `L9-N9` (`L10-N9`), the lines depict `L9-N8`, while the big hatched symbols on small scales are `L9-N10`. Positive (negative) values are indicated as the upward (downward) triangles or the solid (dashed) lines.

At high redshifts, we can see a prominent peak at $k = q$ as expected from linear theory (i.e., no mode transfer). Nonlinear coupling then gradually grows

with time and the peak feature gets less significant. One of the key features here is the larger contribution from smaller wave modes ($q < k$); the growth of structure is dominated by mode flows from large to small scales. Not surprisingly, the formation of a structure is more efficiently amplified when it is part of a larger structure than when it contains small-scale features.

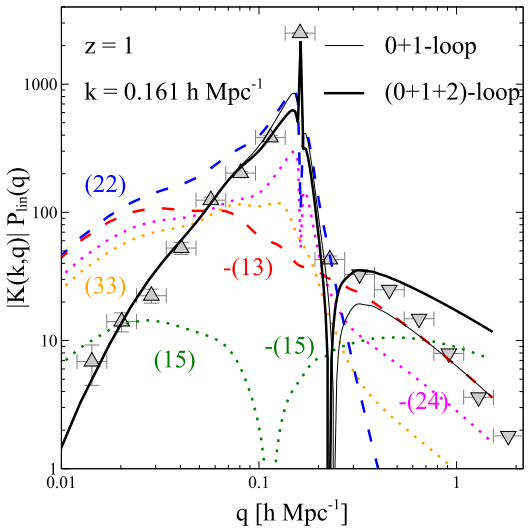

Figure 2: Response function predicted by PT (un-binned) up to one- (thin solid) and two-loop (thick solid) order at $k = 0.161h\,\mathrm{Mpc}^{-1}$ at $z = 1$. Dashed (dotted) lines show each of the one- (two-)loop contributions with the legend (ij) showing the perturbative order of the calculation. We show a negative sign in the legend when K is negative. The simulation data `L9-N9` are also shown by triangles.

Such findings are fully in line with expectations from PT calculations. We show the predictions in Fig. 2 up to the two-loop level (i.e., next-to-next-to-leading order) ignoring binning effects at this stage. We present the contribution from $P_{ij}(k) \propto \langle \delta^{(i)} \delta^{(j)} \rangle$, where $\delta^{(i)}$ is the ith-order overdensity in the PT expansion. The terms at the same loop order cancel at small q due to the galilean invariance of the system as discussed in e.g., [26, 27, 28, 29, 30]. On the other hand, small scales are dominated by one term at each order, $P_{13}(k)$ and $P_{15}(k)$. Similarly, it has been shown that, at the p-loop order in PT, the term originating from the $(2p+1)$th-order density kernel function, F_{2p+1}, dominates the mode-coupling effect from small scales [14].

We then rescale the response function at various redshifts as $T(k,q) = [K(k,q) - K^{\rm lin}(k,q)]/[qP^{\rm lin}(k)]$, where $K^{\rm lin}$ is the linear contribution, and plot them in Fig. 3. They are compared with the one-loop PT calculation (solid), which is time-independent with this normalization. The simulation data indeed show little time dependence at $q \lesssim k$ in remarkable agreement with the one-loop

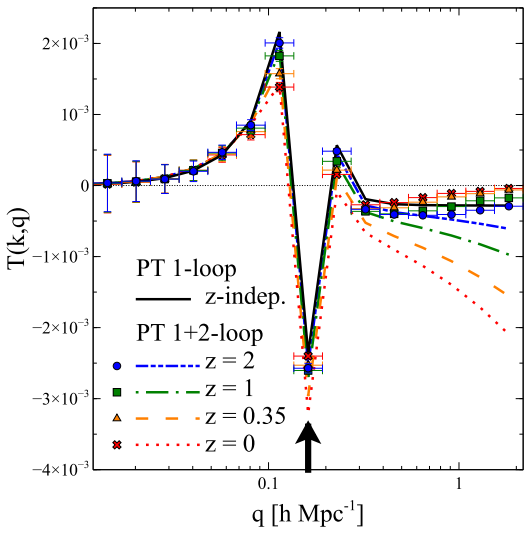

Figure 3: Rescaled response function, $T(k,q) \equiv [K(k,q) - K^{\rm lin}(k,q)]/[qP^{\rm lin}(k)]$. PT calculations are shown by lines, whereas the symbols are `L9-N9` (see legend for detail). The nonlinear wave-mode bin is fixed at $k = 0.161\,h\,{\rm Mpc}^{-1}$ (vertical arrow). Binning is taken into account to the analytical calculations consistently to the simulations.

calculation, reproducing the expected q dependence [9], as well as the change of sign between large and small scales. The small but non-negligible z-dependence at $k \sim q$ is further reproduced by the two-loop calculation (see the figure legend). Note that at the wave-mode k plotted here (i.e., $0.161\,h\,{\rm Mpc}^{-1}$), the two-loop PT prediction for the nonlinear power spectrum agrees with simulations within 1% at $z \gtrsim 1$ and the agreement gets worse at lower redshift reaching to $\sim 5\%$ at $z = 0$ (see e.g., [15]).

At $q \gtrsim 0.3\,h\,{\rm Mpc}^{-1}$, however, the measured response function is damped compared to the PT. The one-loop PT predicts the response function to reach a constant [10]; at the two-loop order, it grows in amplitude with time. The numerical measurements show on the other hand that the scaled response function is strongly damped with decreasing redshift. It is such that the couplings take place effectively between modes of similar wavelengths. This effect is particularly important at late time. At redshift zero, the discrepancy between the model and simulations is striking. Furthermore, analysis of the response structure at three and higher loop order (see e.g., [14]) suggests that PT calculations, at any finite order, predict an even larger amplitude of the response function in the high q region. This strongly suggests that this anomaly is genuinely non-perturbative.

[9] It has the small-q asymptote $[2519/4410 - (23/84)n + (1/20)n^2]q^2/\pi^2$ for an Einstein-de Sitter background, with n being the local slope of the linear spectrum.

[10] This constant is $-61k^2/(630\pi^2)$ for an Einstein-de Sitter background.

We propose an effective description of this observed behavior. As illustrated in Fig. 4 it can be modeled with a Lorentzian:

$$T^{\rm eff.}(k,q) \xrightarrow{\rm high-}{}^{q} T^{1+2-{\rm loop}}(k,q)\frac{1}{1+(q/q_0)^2} \tag{4}$$

characterized by a critical wave mode, q_0, which does not depend on the nonlinear wave mode k. We naively expect that this scale corresponds to the scale at which the fluctuation is order unity and thus pertrubative expansion is not valid. Indeed, we numerically found that a simple fitting formula

$$\sigma_{\rm lin}(R;z)|_{R=1/q_0} = 1.35, \tag{5}$$

where $\sigma^2_{\rm lin}(R)$ is the variance of the linear density fluctuation smoothed with a gaussian filter of the form $\exp[-(0.46kR)^2/2]$ [11], can explain reasonablly well the data points not only for the fiducial model but for the models with different spectral indices (see Fig. 5). One can find that the fit is not as accurate at $z = 1$ for the `low_ns` model, suggesting the limitation of the fitting formula. Nevertheless, a simple form (4) with a single parameter 1.35 in Eq. (5) seems to capture the damping tail of the response function in a rather wide range of cosmological models at different redshifts. Note that, the k-dependence of the responce function at the high-q limit is preserved in perturbative calculations (it is always proportional to k^2 independent of the perturbative order due to the asymptote of the F_n kernel function). The independence of q_0 on k is thus in full agreement with PT predictions.

4. Discussion

The simulation results give a clear evidence that the mode transfer from small to large scales is suppressed compared to the PT prediction when the mode q enters the nonperturbative regime. However, the origin of the suppression is yet to be understood. In particular it is not clear whether this has its roots in shell crossing or not. For instance, we can find in [32] that vorticity and velocity dispersion generated by shell crossing can alter the evolution of density fluctuations through nonlinear coupling. Especially, the latter is shown to give non-negligible corrections to the density power spectrum even on very large ($\sim 0.1h\,{\rm Mpc}^{-1}$) scales. This indicates that multistreaming physics, which take place on small scales, are somehow related to the growth of large-scale fluctuations, and this is exactly the coupling of large and small scales that we discuss here. Effective Field Theory (EFT) approaches as advocated originally in [33, 34, 35] would be a natural framework to invoke for accounting for such multistreaming effects. In these approaches, however, the response function is ultimately encoded in free coefficients for which no theory exists.

[11] The factor 0.46 here is chosen for a better correspondence with the top-hat radius in terms of the variance. See [31] for more detail.

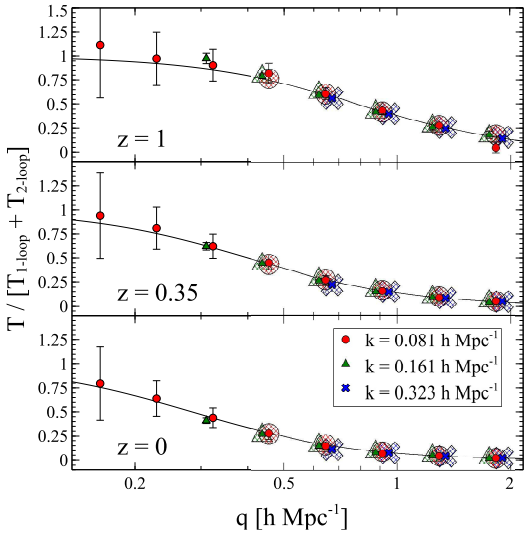

Figure 4: Response function divided by the two-loop PT at the three wave modes k shown in the legend. We plot data points only at $q \geq 2k$ for definiteness. The over-plotted solid lines correspond to the empirical form (4), small solid symbols are `L9-N9` while the big hatched are `L9-N10`.

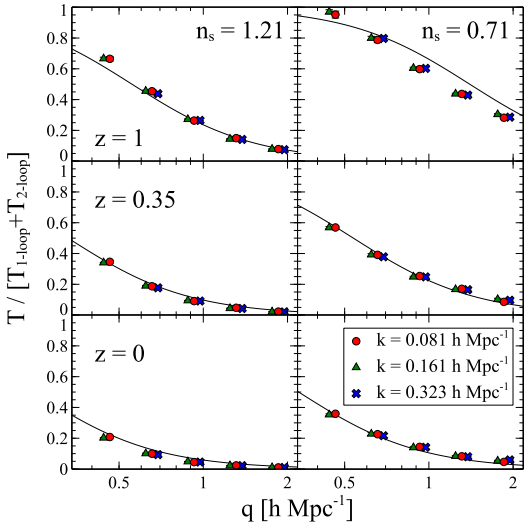

Figure 5: Same as Fig. 4, but for cosmological models with different spectral indices, `high_ns` and `low_ns`.

It might be possible that such damping effect originates from simpler mechanisms in single-stream physics. It has been shown in particular that the nonlinear density propagator, which expresses the evolution of a given wave mode

with time, is exponentially damped by the large-scale displacements. This is the standard result on which the Renormalized Perturbation Theory is based [36, 37]. As explicitly shown in [38] equal-time spectra are however insensitive to displacements of the global system, that originates from wave modes smaller than k. Displacements at intermediate scales are nonetheless expected to induce some effective damping for equal-time spectra. The physical idea behind that is that the force driving the collapse of a large-scale perturbation (e.g., a cluster of galaxies) is affected by the small scale inhomogeneities within the structure (say galaxies), but that this dependence might be damped when such small scale inhomogeneities are actually moving within the structure. It is however beyond the scope of this presentation to evaluate the importance of this effect.

5. Summary

We have presented the first direct measurement of the response function that governs the dependence of the nonlinear power spectrum on the initial spectrum during cosmic structure formation. This measurement was done using a large ensemble of N-body simulations that differ slightly in their initial conditions. The results were found to be robust to the simulation resolution – as shown in Table 1 – supporting the idea that measured shapes were genuine features in the development of gravitational instabilities.

The response functions were computed concurrently at next and next-to-next leading order in PT. Comparisons with measurements show a remarkable agreement over a wide range of scale and time. We found however mode transfers from small to large scales to be strongly suppressed compared to theoretical expectations especially at late time. We propose a description of the damping tail with a Lorentzian shape.

These results are of far-reaching consequences. They first give insights into the mode coupling structure of cosmological fluids and show that PT approaches capture most of their properties. The small scale damping signals the validity limit of the PT beyond next-to-leading order. It provides in particular indications on how to regularize their contributions. The observed damping also marks the irruption of collective non-linear effects although the underlying mechanisms are yet to be uncovered. Most importantly the damped response suggests that small scale physics, whether from the initial metric perturbations or late-time processes, can be effectively controlled. It paves the way for solid estimates of the theoretical uncertainties on the determination of cosmological parameters (such as inflationary primordial non-Gaussianities, neutrino masses or dark energy parameters) from large-scale surveys.

Acknowledgment

We thank Patrick Valageas for fruitful discussions on analytical calculations of the response function. We also thank Yasushi Suto for insightful comments on the origin of our findings. This works is supported in part by grant ANR-12-BS05-0002 of the French Agence Nationale de la Recherche. TN is supported

by JSPS. AT is supported by a Grant-in-Aid for Scientific Research from the Japan Society for the Promotion of Science (JSPS) (No. 24540257). Numerical calculations for the present work have been carried out on Cray XC30 at Center for Computational Astrophysics, CfCA, of National Astronomical Observatory of Japan.

[1] A. Albrecht, G. Bernstein, R. Cahn, W. L. Freedman, J. Hewitt, W. Hu, J. Huth, M. Kamionkowski, E. W. Kolb, L. Knox, J. C. Mather, S. Staggs, N. B. Suntzeff, Report of the Dark Energy Task Force, ArXiv Astrophysics e-printsarXiv:astro-ph/0609591.

[2] G. Hinshaw, D. Larson, E. Komatsu, D. N. Spergel, C. L. Bennett, J. Dunkley, M. R. Nolta, M. Halpern, R. S. Hill, N. Odegard, L. Page, K. M. Smith, J. L. Weiland, B. Gold, N. Jarosik, A. Kogut, M. Limon, S. S. Meyer, G. S. Tucker, E. Wollack, E. L. Wright, Nine-year Wilkinson Microwave Anisotropy Probe (WMAP) Observations: Cosmological Parameter Results, ApJS208 (2013) 19. arXiv:1212.5226, doi:10.1088/0067-0049/208/2/19.

[3] Planck Collaboration, P. A. R. Ade, N. Aghanim, M. Arnaud, M. Ashdown, J. Aumont, C. Baccigalupi, A. J. Banday, R. B. Barreiro, J. G. Bartlett, et al., Planck 2015 results. XIII. Cosmological parameters, ArXiv e-printsarXiv:1502.01589.

[4] D. J. Eisenstein, I. Zehavi, D. W. Hogg, R. Scoccimarro, M. R. Blanton, R. C. Nichol, R. Scranton, H.-J. Seo, M. Tegmark, Z. Zheng, S. F. Anderson, J. Annis, N. Bahcall, J. Brinkmann, S. Burles, F. J. Castander, A. Connolly, I. Csabai, M. Doi, M. Fukugita, J. A. Frieman, K. Glazebrook, J. E. Gunn, J. S. Hendry, G. Hennessy, Z. Ivezić, S. Kent, G. R. Knapp, H. Lin, Y.-S. Loh, R. H. Lupton, B. Margon, T. A. McKay, A. Meiksin, J. A. Munn, A. Pope, M. W. Richmond, D. Schlegel, D. P. Schneider, K. Shimasaku, C. Stoughton, M. A. Strauss, M. SubbaRao, A. S. Szalay, I. Szapudi, D. L. Tucker, B. Yanny, D. G. York, Detection of the Baryon Acoustic Peak in the Large-Scale Correlation Function of SDSS Luminous Red Galaxies, ApJ633 (2005) 560–574. arXiv:arXiv:astro-ph/0501171, doi:10.1086/466512.

[5] S. Cole, W. J. Percival, J. A. Peacock, P. Norberg, C. M. Baugh, C. S. Frenk, I. Baldry, J. Bland-Hawthorn, T. Bridges, R. Cannon, M. Colless, C. Collins, W. Couch, N. J. G. Cross, G. Dalton, V. R. Eke, R. De Propris, S. P. Driver, G. Efstathiou, R. S. Ellis, K. Glazebrook, C. Jackson, A. Jenkins, O. Lahav, I. Lewis, S. Lumsden, S. Maddox, D. Madgwick, B. A. Peterson, W. Sutherland, K. Taylor, The 2dF Galaxy Redshift Survey: power-spectrum analysis of the final data set and cosmological implications, MNRAS362 (2005) 505–534. arXiv:astro-ph/0501174, doi:10.1111/j.1365-2966.2005.09318.x.

[6] N. Kaiser, Clustering in real space and in redshift space, Mon. Not. Roy. Astron. Soc. 227 (1987) 1–21.

[7] E. V. Linder, Redshift distortions as a probe of gravity, Astroparticle Physics 29 (2008) 336–339. arXiv:0709.1113, doi:10.1016/j.astropartphys.2008.03.002.

[8] M. Kilbinger, Review article: Cosmology with cosmic shear observations, ArXiv e-printsarXiv:1411.0115.

[9] Y. P. Jing, P. Zhang, W. P. Lin, L. Gao, V. Springel, The Influence of Baryons on the Clustering of Matter and Weak-Lensing Surveys, ApJL640 (2006) L119–L122. arXiv:astro-ph/0512426, doi:10.1086/503547.

[10] E. Semboloni, H. Hoekstra, J. Schaye, M. P. van Daalen, I. G. McCarthy, Quantifying the effect of baryon physics on weak lensing tomography, MNRAS417 (2011) 2020–2035. arXiv:1105.1075, doi:10.1111/j.1365-2966.2011.19385.x.

[11] I. Mohammed, D. Martizzi, R. Teyssier, A. Amara, Baryonic effects on weak-lensing two-point statistics and its cosmological implications, ArXiv e-printsarXiv:1410.6826.

[12] F. Bernardeau, S. Colombi, E. Gaztañaga, R. Scoccimarro, Large-scale structure of the Universe and cosmological perturbation theory, Phys. Rep. 367 (2002) 1–248. arXiv:arXiv:astro-ph/0112551, doi:10.1016/S0370-1573(02)00135-7.

[13] A. Taruya, F. Bernardeau, T. Nishimichi, S. Codis, Direct and fast calculation of regularized cosmological power spectrum at two-loop order, Physical Review D86 (10) (2012) 103528. arXiv:1208.1191, doi:10.1103/PhysRevD.86.103528.

[14] F. Bernardeau, A. Taruya, T. Nishimichi, Cosmic propagators at two-loop order, Physical Review D89 (2) (2014) 023502. doi:10.1103/PhysRevD.89.023502.

[15] D. Blas, M. Garny, T. Konstandin, Cosmological perturbation theory at three-loop order, JCAP1 (2014) 10. arXiv:1309.3308, doi:10.1088/1475-7516/2014/01/010.

[16] R. E. Angulo, S. D. M. White, V. Springel, B. Henriques, Galaxy formation on the largest scales: the impact of astrophysics on the baryonic acoustic oscillation peak, MNRAS442 (2014) 2131–2144. arXiv:1311.7100, doi:10.1093/mnras/stu905.

[17] F. Prada, C. G. Scoccola, C.-H. Chuang, G. Yepes, A. A. Klypin, F.-S. Kitaura, S. Gottlober, C. Zhao, Hunting down systematics in baryon acoustic oscillations after cosmic high noon, ArXiv e-printsarXiv:1410.4684.

[18] M. C. Neyrinck, L. F. Yang, Ringing the initial Universe: the response of overdensity and transformed-density power spectra to initial spikes, MNRAS433 (2013) 1628–1633. arXiv:1305.1629, doi:10.1093/mnras/stt949.

[19] E. Komatsu, J. Dunkley, M. R. Nolta, C. L. Bennett, B. Gold, G. Hinshaw, N. Jarosik, D. Larson, M. Limon, L. Page, D. N. Spergel, M. Halpern, R. S. Hill, A. Kogut, S. S. Meyer, G. S. Tucker, J. L. Weiland, E. Wollack, E. L. Wright, Five-Year Wilkinson Microwave Anisotropy Probe Observations: Cosmological Interpretation, Astrophys. J. Suppl. 180 (2009) 330–376. arXiv:0803.0547, doi:10.1088/0067-0049/180/2/330.

[20] A. Lewis, A. Challinor, A. Lasenby, Efficient Computation of Cosmic Microwave Background Anisotropies in Closed Friedmann-Robertson-Walker Models, Astrophys. J. 538 (2000) 473–476. arXiv:astro-ph/9911177, doi:10.1086/309179.

[21] T. Nishimichi, A. Shirata, A. Taruya, K. Yahata, S. Saito, Y. Suto, R. Takahashi, N. Yoshida, T. Matsubara, N. Sugiyama, I. Kayo, Y. Jing, K. Yoshikawa, Modeling Nonlinear Evolution of Baryon Acoustic Oscillations: Convergence Regime of N-body Simulations and Analytic Models, Publ. Astron. Soc. Japan 61 (2009) 321–. arXiv:0810.0813.

[22] P. Valageas, T. Nishimichi, Combining perturbation theories with halo models, Astronomy & Astrophysics 527 (2011) A87. arXiv:1009.0597, doi:10.1051/0004-6361/201015685.

[23] R. Scoccimarro, Transients from initial conditions: a perturbative analysis, Mon. Not. Roy. Astron. Soc. 299 (1998) 1097–1118. arXiv:arXiv:astro-ph/9711187, doi:10.1046/j.1365-8711.1998.01845.x.

[24] M. Crocce, S. Pueblas, R. Scoccimarro, Transients from initial conditions in cosmological simulations, Mon. Not. Roy. Astron. Soc. 373 (2006) 369–381. arXiv:astro-ph/0606505, doi:10.1111/j.1365-2966.2006.11040.x.

[25] V. Springel, The cosmological simulation code GADGET-2, Mon. Not. Roy. Astron. Soc. 364 (2005) 1105–1134. arXiv:astro-ph/0505010, doi:10.1111/j.1365-2966.2005.09655.x.

[26] B. Jain, E. Bertschinger, Self-similar Evolution of Gravitational Clustering: Is N = -1 Special?, ApJ456 (1996) 43. arXiv:astro-ph/9503025, doi:10.1086/176625.

[27] R. Scoccimarro, J. Frieman, Loop Corrections in Nonlinear Cosmological Perturbation Theory, ApJS105 (1996) 37. arXiv:astro-ph/9509047, doi:10.1086/192306.

[28] M. Peloso, M. Pietroni, Galilean invariance and the consistency relation for the nonlinear squeezed bispectrum of large scale structure, JCAP5 (2013) 31. arXiv:1302.0223, doi:10.1088/1475-7516/2013/05/031.

[29] A. Kehagias, A. Riotto, Symmetries and consistency relations in the large scale structure of the universe, Nuclear Physics B 873 (2013) 514–529. arXiv:1302.0130, doi:10.1016/j.nuclphysb.2013.05.009.

[30] D. Blas, M. Garny, T. Konstandin, On the non-linear scale of cosmological perturbation theory, JCAP9 (2013) 24. arXiv:1304.1546, doi:10.1088/1475-7516/2013/09/024.

[31] A. Paranjape, R. K. Sheth, V. Desjacques, Excursion set peaks: a self-consistent model of dark halo abundances and clustering, MNRAS431 (2013) 1503–1512. arXiv:1210.1483, doi:10.1093/mnras/stt267.

[32] S. Pueblas, R. Scoccimarro, Generation of vorticity and velocity dispersion by orbit crossingarXiv:0809.4
URL https://arxiv.org/abs/0809.4606

[33] D. Baumann, A. Nicolis, L. Senatore, M. Zaldarriaga, Cosmological non-linearities as an effective fluid, JCAP7 (2012) 51. arXiv:1004.2488, doi:10.1088/1475-7516/2012/07/051.

[34] J. J. M. Carrasco, M. P. Hertzberg, L. Senatore, The effective field theory of cosmological large scale structures, Journal of High Energy Physics 9 (2012) 82. arXiv:1206.2926, doi:10.1007/JHEP09(2012)082.

[35] M. P. Hertzberg, Effective field theory of dark matter and structure formation: Semianalytical results, Physical Review D89 (4) (2014) 043521. arXiv:1208.0839, doi:10.1103/PhysRevD.89.043521.

[36] M. Crocce, R. Scoccimarro, Renormalized cosmological perturbation theory, Physical Review D73 (6) (2006) 063519. arXiv:arXiv:astro-ph/0509418, doi:10.1103/PhysRevD.73.063519.

[37] M. Crocce, R. Scoccimarro, Memory of initial conditions in gravitational clustering, Physical Review D73 (6) (2006) 063520. arXiv:astro-ph/0509419, doi:10.1103/PhysRevD.73.063520.

[38] F. Bernardeau, N. van de Rijt, F. Vernizzi, Resummed propagators in multicomponent cosmic fluids with the eikonal approximation, Physical Review D85 (6) (2012) 063509. arXiv:1109.3400, doi:10.1103/PhysRevD.85.063509.